

Article

Not peer-reviewed version

---

# Analysis of the Optical Properties and Electronic Structure of Semiconductors of the $\text{Cu}_2\text{NiXS}_4$ ( $X = \text{Si, GE, Sn}$ ) Family as New Promising Materials for Optoelectronic Devices

---

[Dilshod Nematov](#) \*

Posted Date: 4 January 2024

doi: 10.20944/preprints202401.0416.v1

Keywords: bandgap; kesterites; optical properties; solar cells; absorption coefficient; dielectric constant; photoelectric applications



Preprints.org is a free multidiscipline platform providing preprint service that is dedicated to making early versions of research outputs permanently available and citable. Preprints posted at Preprints.org appear in Web of Science, Crossref, Google Scholar, Scilit, Europe PMC.

Copyright: This is an open access article distributed under the Creative Commons Attribution License which permits unrestricted use, distribution, and reproduction in any medium, provided the original work is properly cited.

Article

# Analysis of the Optical Properties and Electronic Structure of Semiconductors of the $\text{Cu}_2\text{NiXS}_4$ ( $X = \text{Si, Ge, Sn}$ ) Family as New Promising Materials for Optoelectronic Devices

Dilshod Nematov

S.U. Umarov Physical-Technical Institute of the NAS Tajikistan, Dushanbe, 734042, Tajikistan; dilnem@phti.ru

**Abstract:** In this work, the optoelectronic characteristics of kesterites of the  $\text{Cu}_2\text{NiXS}_4$  system ( $X = \text{Si, Ge, Sn}$ ) were studied. The electronic properties of the  $\text{Cu}_2\text{NiXS}_4$  ( $X = \text{Si, Ge, Sn}$ ) system were studied using first-principles calculations within the framework of density functional theory. For calculations, ab initio codes VASP and Wien2k were used. The high-precision modified Beke-Jones (mBJ) functional and the hybrid HSE06 functional were used to estimate the bandgap, electronic and optical properties. Calculations have shown that when replacing Si with Ge and Sn, the band gap decreases from 2.58 eV to 1.33 eV. Replacing Si with Ge and Sn reduces the overall density of electronic states. In addition, new deep (shallow) states are formed in the band gap of these crystals, which is confirmed by the behavior of their optical properties. The obtained band gap values are compared with existing experimental measurements, demonstrating good agreement between HSE06 calculations and experimental data. The nature of changes in the dielectric constant, absorption capacity and optical conductivity of these systems depending on the photon energy has also been studied. The statistical dielectric constant and refractive index of these materials were found. The results will help increase the amount of information about the properties of the materials under study and will allow the use of these compounds in a wider range of optoelectronic devices, in particular, in solar cells and other devices that use solar radiation to generate electric current.

**Keywords:** bandgap; kesterites; optical properties; solar cells; absorption coefficient; dielectric constant; photoelectric applications

## 1. Introduction

One of the factors contributing to global warming is the burning of fossil fuels, which increases the concentration of carbon dioxide in the atmosphere, warming the planet and changing the climate [1–3]. The Earth absorbs a significant portion of the light emitted by the Sun when it reaches its surface. As a result of heating the planet with this energy, its surface emits infrared radiation. The greenhouse effect, which causes global warming, occurs when carbon dioxide in the atmosphere absorbs much of the incoming thermal radiation and reflects it back to the Earth's surface [4,5]. It is known that electricity generation emits about 40% of greenhouse gases into the atmosphere [6,7]. However, the world now obtains 80% of its energy from fossil fuels (oil, coal, and gas), which also contribute to environmental pollution and the daily depletion of these natural supplies [8]. Thus, in light of the anticipated need for electricity worldwide and the 21st - century green energy agenda, the issue of the development of alternative and renewable energy sources is brought up, and the potential for transforming non-traditional energy into electricity is examined [9].

Alternative sources such as windmills, moisture-to-electricity converters, thermoelectric (TE) generators, photovoltaic (PV) converters (solar panels), solar thermophotovoltaic converters and the use of geothermal waters have a positive effect on the air environment, but they are not available everywhere. One of the effective natural sources of alternative energy is the synthesis and

optimization of the properties of new nanomaterials to create solar energy converters into electricity, which is very effective and environmentally friendly compared to many other methods [1–9]. The great growth potential of this alternative energy industry is due to such global factors as the need to ensure national energy security and the rising cost of fossil energy sources. Alternative energy has other unique advantages: for example, solar energy is available to everyone, free, practically inexhaustible, and the process of converting it into electrical energy does not have a negative impact on the environment [10–13].

In recent years, photovoltaics has been rapidly developing for the developed of which, in addition to silicon and perovskites, many types of crystalline materials have been developed and proposed [14–21]. One of these promising and promising materials is kesterite materials with the general formula  $A_2BCD_4$  ( $A = \text{Cu, Ag}$ ;  $B = \text{Zn, Cd, Ni, Mg, ...}$ ;  $C = \text{Sn, Ge, Si}$ ;  $D = \text{S, Se}$ ) [22]. Since their emergence as so-called “Third generation generators,” photovoltaic (PV) systems have been hailed as an environmentally and economically viable alternative to conventional technologies for solving the world’s energy, safety and environmental problems [23–25]. However, despite the obvious achievements in this area, the development and research of the fundamental properties of potentially new kesterite photovoltaic materials is of great importance for improving the performance of devices based on them.

Because of their direct bandgap in the 1.0–2.5 eV region, the most extensively used kesterite crystals based on the  $\text{Cu}_2\text{ZnSnS}_4$  and  $\text{Cu}_2\text{ZnSnSe}_4$  (CZTSSe) system are utilized in the industrial manufacture of solar panels [26]. Kesterite’s range of use is increased by the adjustable band gap, which also enables task-specific adjustment for ideal spectral matching [27]. Furthermore, they are excellent candidates for the production of solar energy due to their p-type conductivity and high optical absorption coefficient ( $>10^4 \text{ cm}^{-1}$ ) [28]. Additionally, this allows for the kesterite film to be thinned down to a point where the solar panel’s cost can be decreased without sacrificing efficiency [28]. The efficiency of kesterite-based solar cells has recently risen from 12.6% to 13.6% [29–31]. However, the performance of solar cells based on this material is still far from the theoretical limit, indicating that the efficiency potential of kesterite is still little exploited. The reason for the poor performance of CZTSSe is mainly due to their high open circuit voltage deficit, which has been repeatedly reported in research papers [32–35]. This is due to fluctuations in the band gap and potential induced by crystalline disorder between elements A and B sites of kesterite which occurs at the structural and electronic levels [32–35]. Existing problems force researchers to develop new analogues of CZTSSe, however, obtaining new perovskites including some members of the  $\text{Cu}_2\text{NiXS}_4$  family ( $X = \text{Si, Ge, Sn}$ ) is labor-intensive work due to the complex single-phase growth of kesterite while obtaining a homogeneous and high-quality layer free of secondary phases [34,35]. Sometimes the final synthesis of kesterite materials results in many undesirable solid solutions, which complicate the work [36], and some resulting materials with a kesterite structure may have undesirable properties. Therefore, in recent years, preliminary prediction of properties applied to the synthesis of materials has become an integral tradition among the solid state community.

In this regard, recently the properties of kesterites have also been studied by various theoretical methods, as a result of which the efficiency of solar cells based on them is constantly increasing [25–36]. Density functional theory (DFT) is a potent theoretical approach that has gained significant traction in the last ten years as a major tool for the theoretical study of solid materials. Its potent approach accounts for the behavior of electrons in all atomic-molecular environments and offers a highly accurate reformulation of quantum mechanical calculations of solids. This is because contemporary computing clusters can solve the Kohn-Sham equations efficiently [37–45]. However, these formulas are predicated on a single estimate, that of the exchange-correlation energy, which accounts for the precision of quantum computations. Here, many of the basic characteristics of compounds based on the  $\text{Cu}_2\text{NiXS}_4$  ( $X = \text{Si, Ge, Sn}$ ) family still remain poorly studied and correspond to the current topic requiring in-depth research, despite the annual increase in publications devoted to the study of the properties of kesterites.

In this work, using quantum chemical calculations within the framework of density functional theory, the electronic and optical properties of kesterites of the  $\text{Cu}_2\text{NiXS}_4$  ( $X = \text{Si, Ge, Sn}$ ) family are

studied, a detailed study and disclosure of which is important for the appropriate selection of the synthesized material for specific applications.

## 2. Materials and methods

Ab initio quantum chemical calculations within the framework of density functional theory were carried out on the basis of data on crystal lattices published in [46], obtained after complete relaxation of lattice parameters using the VASP package [47] and the SCAN functional [48–50]. In this case, electronic and ion relaxation was achieved at a cutoff energy of 550 eV and  $3 \times 3 \times 3$  k-points. The band gap, electronic structure and optical properties of  $\text{Cu}_2\text{NiXS}_4$  ( $X = \text{Si}, \text{Ge}, \text{Sn}$ ) systems were studied using the VASP and Wien2k quantum chemical simulation codes using the hybrid functional HSE06 [51] and the modified TB-mBJ functional [52]. The optimal plane wave cutoff value  $K_{\text{max}}$  was selected as  $6.0 \text{ Ry}^{1/2}$ . The Kohn-Sham equations were solved using LAPW. Kesterite crystals of the tetragonal system (symmetry group I-4) were chosen as the structures under study. The following valence electrons were considered: Si:  $3s^2 3p^2$ , Cu:  $3d^{10} 4s^1$ , Sn:  $4d^{10} 5s^2 5p^2$ , Ni:  $3d^{10} 4s^2$ , Ge:  $3d^{10} 4s^2 4p^2$ , and S:  $3s^2 3p^4$ .

## 3. Results and discussion

The energy band distribution diagram, the band energy's dependence on the density of electronic states (DOS), and the band gap's numerical values are used to evaluate the electronic characteristics of the  $\text{Cu}_2\text{NiXS}_4$  ( $X = \text{Si}, \text{Ge}, \text{and Sn}$ ) system. Table 1 compares the bandgap values we calculated within DFT - HSE06 with the results of experimental measurements by independent authors.

**Table 1.** Comparison of the calculated value of the band gap of the  $\text{Cu}_2\text{NiSiS}_4$ ,  $\text{Cu}_2\text{NiGeS}_4$ ,  $\text{Cu}_2\text{NiSnS}_4$  system with literature data.

	Bandgap, eV		
	THIS WORK		LITERATURE
	HSE06	Calc.	Experimental
$\text{Cu}_2\text{NiSiS}_4$	2.560	-	-
$\text{Cu}_2\text{NiGeS}_4$	1.802	1.13[53]	1.8 [53]
$\text{Cu}_2\text{NiSnS}_4$	1.321	1.26[54]	1.31 [55], 1.38 [56]

As shown in Table 1, the results of bandgap calculations of  $\text{Cu}_2\text{NiSnS}_4$ ,  $\text{Cu}_2\text{NiGeS}_4$  crystals obtained from the HSE06 functional are in good agreement with experiment.

The total density of electronic states of  $\text{Cu}_2\text{NiSnS}_4$ ,  $\text{Cu}_2\text{NiGeS}_4$ , and  $\text{Cu}_2\text{NiSiS}_4$  semiconductor crystals were then analyzed using mBJ calculations. The results of calculations of the total density of electronic states for  $\text{Cu}_2\text{NiSnS}_4$ ,  $\text{Cu}_2\text{NiGeS}_4$ , and  $\text{Cu}_2\text{NiSiS}_4$  crystals are shown in Figure 1a–c.

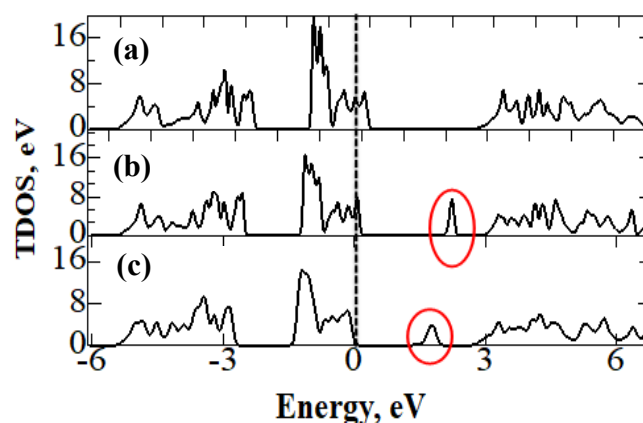


**Figure 1.** Total density of electronic states for  $\text{Cu}_2\text{NiSiS}_4$  (a),  $\text{Cu}_2\text{NiGeS}_4$  (b) and  $\text{Cu}_2\text{NiSnS}_4$  (c).

The results shown in Figure 2 demonstrate that the band gap lowers and the Fermi levels move towards the valence band when Si is substituted with Ge and Sn. Conversely, it is evident that the density of states drops when Sn takes the place of Si. In this case, new electronic states are formed in the energy gap of  $\text{Cu}_2\text{NiGeS}_4$  and  $\text{Cu}_2\text{NiSnS}_4$ , which are important from the point of view of using the material in electronic devices.

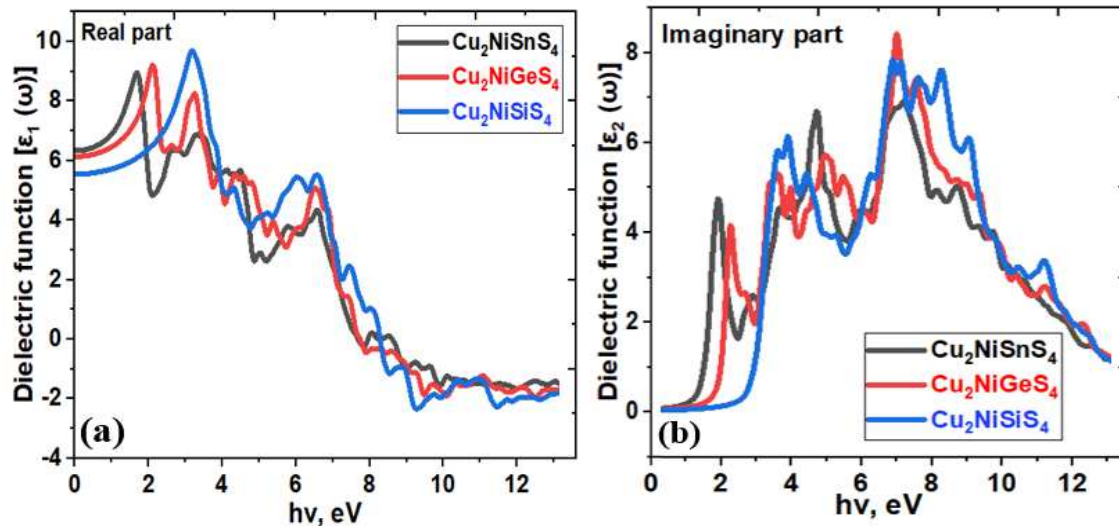


**Figure 2.** Real (a) and imaginary part (b) dielectric constant of kesterites of the  $\text{Cu}_2\text{NiXS}_4$  ( $X = \text{Si}, \text{Ge}, \text{Sn}$ ) family.

To justify the change in the bandgap width, it is necessary to analyze the spectra of the optical properties of the materials under study. Calculated optical properties of materials, including their absorption coefficient and refractive index, provide information about what type of response these materials will exhibit when photons are incident on them [57]. The optical properties of the  $\text{Cu}_2\text{NiXS}_4$  ( $X = \text{Si}, \text{Ge}, \text{Sn}$ ) system were investigated based on the calculation of their real ( $\epsilon_1$ ) and imaginary ( $\epsilon_2$ ) parts of the dielectric functions. The real part shows the energy-saving capacity of a material, which is something that is assumed to be inherent in all materials at zero energy or zero frequency limit. Figure 2a,b shows the curves of  $\epsilon_1$  and  $\epsilon_2$  versus the energy of incident photons for kesterites of the  $\text{Cu}_2\text{NiXS}_4$  ( $X = \text{Si}, \text{Ge}, \text{Sn}$ ) family.

From Figure 2a it can be seen that at the highest photon energies, all these materials, namely kesterite containing silicon, exhibit metallic behavior. That is, a negative value of the real part indicates the possession of a metallic nature at high energies. This makes it possible to estimate the metallicity fractions of materials using a real function, which shows feedback from the optical band gap. For solar devices, the behavior of these materials indicates the energy gain, whereas the imaginary component of the dielectric function indicates the compound's absorptive capacity. This provides information about how the material reacts when exposed to electromagnetic radiation [58–61]. According to Figure 2b, the replacement of Si with Ge and Sn leads to an increase in the absorption coefficient of the materials under study in the IR and visible radiation range, which is important for the use of materials in solar panels.

The results displayed in Figure 3 make it evident that adding germanium and tin in place of silicon raises the  $\text{Cu}_2\text{NiXS}_4$  ( $X = \text{Si}, \text{Ge}, \text{Sn}$ ) system's refractive index ( $n$ ). In some energy ranges, the refractive index falls drastically below unity after reaching its maximum value. Furthermore, we can deduce from the expression  $n=c/v$  that a refractive index value less than one means that the incident radiation's phase velocity is greater than  $c$ , which allows the incident rays to pass through the material and turn it transparent to incoming radiation [62,63]. Table 2 shows the static values of  $\epsilon_1^*(0)$ ,  $\epsilon_2^*(0)$  and  $n$  according to the DFT-mBJ-WIEN2k calculations.

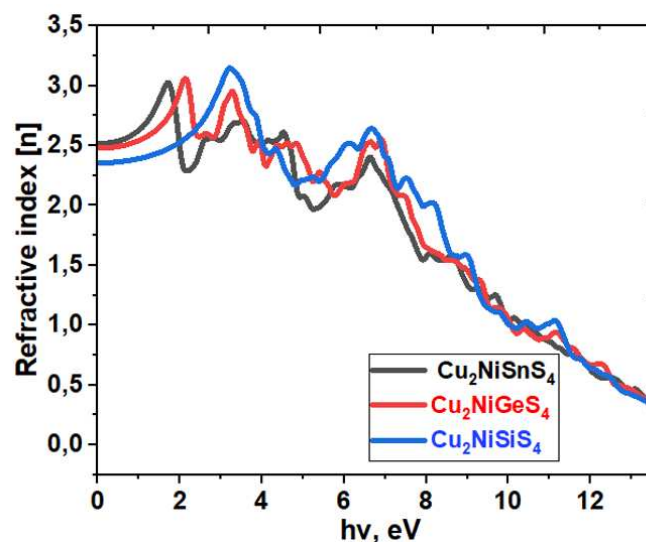


**Figure 3.** Calculated refractive index spectra of the  $\text{Cu}_2\text{NiXS}_4$  ( $X = \text{Si, Ge, Sn}$ ) system as a function of photon energy.

**Table 2.** Calculated values of statistical dielectric constant and refractive index for kesterites of the  $\text{Cu}_2\text{NiXS}_4$  ( $X = \text{Si, Ge, Sn}$ ) family.

System	$\epsilon_1^x(0)$	$\epsilon_2^z(0)$	$n$
$\text{Cu}_2\text{NiSiS}_4$	5.68	5.61	2.52
$\text{Cu}_2\text{NiGeS}_4$	6.11	6.46	2.48
$\text{Cu}_2\text{NiXS}_4$	6.46	6.88	2.36

Beyond the Fermi level, it is known that photon absorption excites occupied states toward unoccupied states. It is known as “optical conduction” when the photons cross the interband transition and as “interband absorption” when they are absorbed. When light is subjected to an electric field, conductivity is known as optical conductivity. Figures 4 and 5 display the computed spectra of the real and imaginary components of the optical conductivity of the systems that are being studied. It is also evident from these spectra that adding Ge and Sn to Si results in improved photoconductivity.

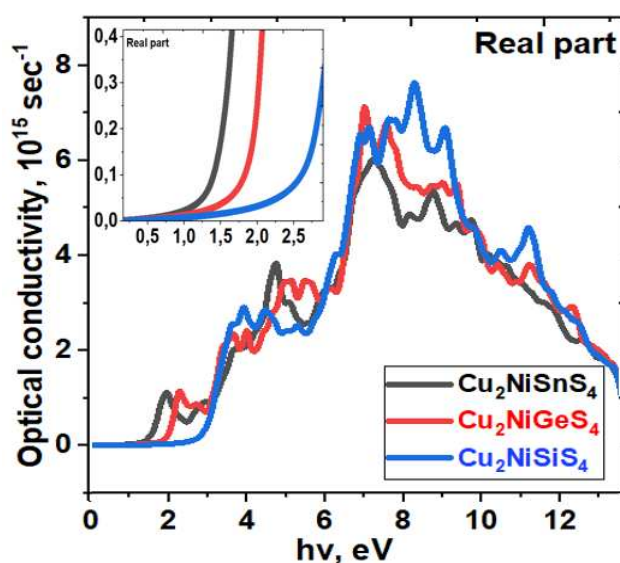


**Figure 4.** Photon energy-dependent spectra of the real part of the optical conductivity of the  $\text{Cu}_2\text{NiXS}_4$  ( $X = \text{Si, Ge, Sn}$ ) system.

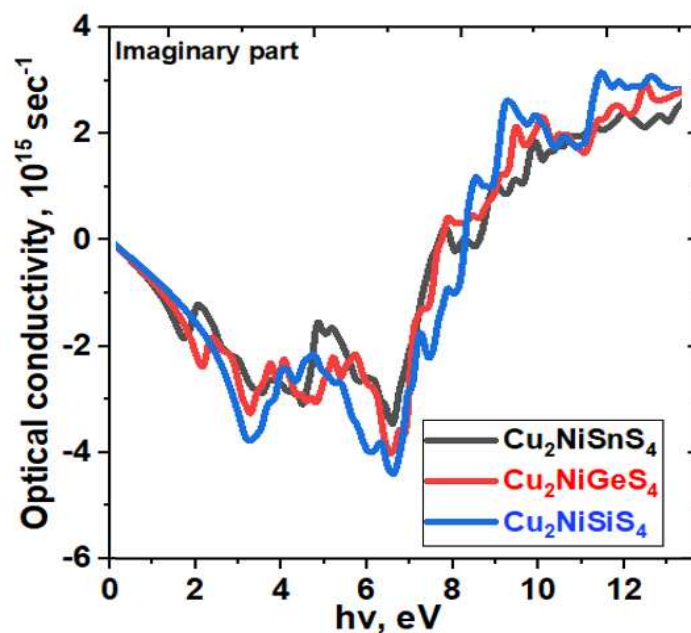


**Figure 5.** Energy-dependent spectra of the imaginary part of the optical conductivity of photons of the  $\text{Cu}_2\text{NiXS}_4$  ( $X = \text{Si}, \text{Ge}, \text{Sn}$ ) system.

Judging by Figures 4 and 5, optical conductivity for the  $\text{Cu}_2\text{NiGeS}_4$  and  $\text{Cu}_2\text{NiSnS}_4$  system begins at energies lower than in the case of  $\text{Cu}_2\text{NiSiS}_4$ . From the data shown in Figure 5, it is clear that all these materials actively absorb light even at low photon energies, namely  $\text{Cu}_2\text{NiSnS}_4$  is sensitive even to rays with an energy of 0.7 eV.  $\text{Cu}_2\text{NiSiS}_4$  also begins to be activated in the energy range above 1.3 eV, having the highest photoconductivity when absorbing short-wavelength radiation [64–69].

## Conclusion

The mBJ exchange correlation potential is employed in this study to simulate the electrical and optical characteristics of  $\text{Cu}_2\text{NiXS}_4$  ( $X = \text{Si}, \text{Ge}, \text{Sn}$ ). Even though the  $\text{Cu}_2\text{NiXS}_4$  ( $X = \text{Si}, \text{Ge}, \text{and Sn}$ ) system's members differ in composition and structure, the permittivity curves and primary optical spectra of all of them exhibit very comparable properties in the infrared and visible radiation ranges. The optical absorption coefficient ( $>10^4 \text{ cm}^{-1}$ ) in the infrared and visible light energy ranges has been discovered to be relatively substantial, and it is proportional to the imaginary part of the permittivity.

**Financial Support:** The work was supported financially by the International Foundation for Humanitarian Cooperation of the CIS within the framework of a scientific project at the expense of a grant from the International Innovation Center for Nanotechnologies of the CIS (GRANT No. 23-112).

## References

- Whiteside, Mark, and J. Marvin Herndon. "Humic like substances (HULIS): Contribution to global warming and stratospheric ozone depletion." *European Journal of Applied Sciences*–Vol 11.2 (2023).
- Jones, Matthew W., et al. "National contributions to climate change due to historical emissions of carbon dioxide, methane, and nitrous oxide since 1850." *Scientific Data* 10.1 (2023): 155
- Voumik, Liton Chandra, et al. "An investigation into the primary causes of carbon dioxide releases in Kenya: Does renewable energy matter to reduce carbon emission?." *Renewable Energy Focus* 47 (2023): 100491.
- Andrews, Steven S. "Thermal Radiation." *Light and Waves: A Conceptual Exploration of Physics*. Cham: Springer International Publishing, 2023. 307-328.
- Weart, Spencer R. "Are There Simple Models of Global Warming?." *The Physics Teacher* 61.6 (2023): 516-518.

6. Aakko-Saksa, Päivi T., et al. "Reduction in greenhouse gas and other emissions from ship engines: Current trends and future options." *Progress in Energy and Combustion Science* 94 (2023): 101055.
7. Voumik, Liton Chandra, et al. "CO<sub>2</sub> emissions from renewable and non-renewable electricity generation sources in the G7 countries: static and dynamic panel assessment." *Energies* 16.3 (2023): 1044
8. Sinclair, Upton. "This Fossil Fuel Project Is Essential." *The Citizen's Guide to Climate Success: Overcoming Myths that Hinder Progress* (2020): 76.
9. Kumar, Arun, and Sandhya Prajapati. *Solar Powered Wastewater Recycling*. CRC Press, 2023.
10. Zhang, Yue, et al. "Advancements in the energy-efficient brine mining technologies as a new frontier for renewable energy." *Fuel* 335 (2023): 127072.
11. Yang, Yuqing, et al. "Modelling and optimal energy management for battery energy storage systems in renewable energy systems: A review." *Renewable and Sustainable Energy Reviews* 167 (2022): 112671.
12. Fraser, Timothy, Andrew J. Chapman, and Yosuke Shigetomi. "Leapfrogging or lagging? Drivers of social equity from renewable energy transitions globally." *Energy Research & Social Science* 98 (2023): 103006.
13. Sayed, Enas Taha, et al. "Recent progress in renewable energy based-desalination in the Middle East and North Africa MENA region." *Journal of Advanced Research* 48 (2023): 125-156.
14. Luceño-Sánchez, José Antonio, Ana María Díez-Pascual, and Rafael Peña Capilla. "Materials for photovoltaics: State of art and recent developments." *International journal of molecular sciences* 20.4 (2019): 976.
15. Huang, Yi-Teng, et al. "Perovskite-inspired materials for photovoltaics and beyond—from design to devices." *Nanotechnology* 32.13 (2021): 132004.
16. Yao, Hui Feng, et al. "Recent progress in chlorinated organic photovoltaic materials." *Accounts of Chemical Research* 53.4 (2020): 822-832.
17. Almora, Osbel, et al. "Device performance of emerging photovoltaic materials (Version 3)." *Advanced energy materials* 13.1 (2023): 2203313.
18. Josephine, Egwunyenga N., Okunzuwa S. Ikponmwoza, and Imosobomeh L. Ikhioya. "Synthesis of SnS/SnO nanostructure material for photovoltaic application." *East European Journal of Physics* 1 (2023): 154-161.
19. Bellucci, A., et al. "Hybrid thermionic-photovoltaic converter with an In<sub>0.53</sub>Ga<sub>0.47</sub>As anode." *Solar Energy Materials and Solar Cells* 238 (2022): 111588.
20. Rafin, SM Sajjad Hossain, Roni Ahmed, and Osama A. Mohammed. "Wide Band Gap Semiconductor Devices for Power Electronic Converters." *2023 Fourth International Symposium on 3D Power Electronics Integration and Manufacturing (3D-PEIM)*. IEEE, 2023.
21. Dada, Modupeola, et al. "Functional materials for solar thermophotovoltaic devices in energy conversion applications: a review." *Frontiers in Energy Research* 11 (2023): 1124288.
22. Chen, Shiyu, et al. "Intrinsic point defects and complexes in the quaternary kesterite semiconductor Cu<sub>2</sub>ZnSnS<sub>4</sub>." *Physical Review B* 81.24 (2010): 245204.
23. Chen, Shiyu, et al. "Defect physics of the kesterite thin-film solar cell absorber Cu<sub>2</sub>ZnSnS<sub>4</sub>." *Applied Physics Letters* 96.2 (2010).
24. Steinhagen, Chet, et al. "Synthesis of Cu<sub>2</sub>ZnSnS<sub>4</sub> nanocrystals for use in low-cost photovoltaics." *Journal of the American Chemical Society* 131.35 (2009): 12554-12555.
25. Chen, S., et al. Recent progress in the theoretical study of Cu<sub>2</sub>ZnSnS<sub>4</sub> and related chalcogenide semiconductors, *Physics*, - 2011, 40, 248-258.
26. Persson, Clas. "Electronic and optical properties of Cu<sub>2</sub>ZnSnS<sub>4</sub> and Cu<sub>2</sub>ZnSnSe<sub>4</sub>." *Journal of Applied Physics* 107.5 (2010).
27. Haight, Richard, Wilfried Haensch, and Daniel Friedman. "Solar-powering the Internet of Things." *Science* 353.6295 (2016): 124-125.
28. Fan, Ping, et al. "High-efficiency ultra-thin Cu<sub>2</sub>ZnSnS<sub>4</sub> solar cells by double-pressure sputtering with spark plasma sintered quaternary target." *Journal of Energy Chemistry* 61 (2021): 186-194.
29. Green, Martin A., et al. Solar cell efficiency tables (version 62). No. NREL/JA-5900-86382. National Renewable Energy Laboratory (NREL), Golden, CO (United States), 2023.
30. NREL, Best Research-Cell Efficiencies, <https://www.nrel.gov/pv/assets/pdfs/cell-pv-eff-emergingpv-rev210726.pdf> (accessed: October 2022).
31. Y. Gong, Q. Zhu, B. Li, S. Wang, B. Duan, L. Lou, C. Xiang, E. Jedlicka, R. Giridharagopal, Y. Zhou, Q. Dai, W. Yan, S. Chen, Q. Meng, H. Xin, *Nat. Energy* 2022, 7, 966.
32. Gupta, G. K., Chaurasiya, R., & Dixit, A. (2019). Theoretical studies on structural, electronic and optical properties of kesterite and stannite Cu<sub>2</sub>ZnGe (S/Se) 4 solar cell absorbers. *Computational Condensed Matter*, 19, e00334.
33. Baid, Mitisha, et al. "A comprehensive review on Cu<sub>2</sub>ZnSnS<sub>4</sub> (CZTS) thin film for solar cell: forecast issues and future anticipation." *Optical and Quantum Electronics* 53 (2021): 1-45.

34. Sahu, Meenakshi, et al. "Review article on the lattice defect and interface loss mechanisms in kesterite materials and their impact on solar cell performance." *Solar Energy* 230 (2021): 13-58.
35. Pu, A. (2018). *Modelling & simulations of Cu<sub>2</sub>ZnSnS<sub>4</sub> thin film solar cell devices* (Doctoral dissertation, UNSW Sydney).
36. Gao, Yuanhao, et al. "Facile non-injection synthesis of high quality CZTS nanocrystals." *RSC Advances* 4.34 (2014): 17667-17670.
37. Banerjee, A. S., Elliott, R. S., & James, R. D. (2015). A spectral scheme for Kohn–Sham density functional theory of clusters. *Journal of Computational Physics*, 287, 226-253.
38. Kato, T., & Saito, S. (2023). Kohn–Sham potentials by an inverse Kohn–Sham equation and accuracy assessment by virial theorem. *Journal of the Chinese Chemical Society*, 70(3), 554-569.
39. Nematov, D. Influence of Iodine Doping on the Structural and Electronic Properties of CsSnBr<sub>3</sub>. *Int. J. Appl. Phys.* 2022, 7, 36–47.
40. Nematov, D.; Kholmurodov, K.; Yuldasheva, D.; Rakhmonov, K.; Khojakhonov, I. Ab-initio Study of Structural and Electronic Properties of Perovskite Nanocrystals of the CsSn[Br<sub>1-x</sub>I<sub>x</sub>]<sub>3</sub> Family. *HighTech Innov. J.* 2022, 3, 140–150.
41. Davlatshoevich, N.D. Investigation Optical Properties of the Orthorhombic System CsSnBr<sub>3-x</sub>I<sub>x</sub>: Application for Solar Cells and Optoelectronic Devices. *J. Hum. Earth Futur.* 2021, 2, 404–411.
42. Dilshod, N.; Kholmirzo, K.; Aliona, S.; Kahramon, F.; Viktoriya, G.; Tamerlan, K. On the Optical Properties of the Cu<sub>2</sub>ZnSn[S<sub>1-x</sub>Se<sub>x</sub>]<sub>4</sub> System in the IR Range. *Trends Sci.* 2023, 20, 4058–4058.
43. Zhang, Yijia, Shujie Zhou, and Kaiwen Sun. "Cu<sub>2</sub>ZnSnS<sub>4</sub> (CZTS) for Photoelectrochemical CO<sub>2</sub> Reduction: Efficiency, Selectivity, and Stability." *Nanomaterials* 13.20 (2023): 2762.
44. Nematov, D. D., Kholmurodov, K. T., Husenzoda, M. A., Lyubchyk, A., & Burhonzoda, A. S. (2022). Molecular Adsorption of H<sub>2</sub>O on TiO<sub>2</sub> and TiO<sub>2</sub>:Y Surfaces. *Journal of Human, Earth, and Future*, 3(2), 213-222.
45. Nematov, D. D., et al. "Molecular Dynamics of DNA Damage and Conformational Behavior on a Zirconium-Dioxide Surface." *Journal of Surface Investigation: X-Ray, Synchrotron and Neutron Techniques* 13.6 (2019): 1165-1184.
46. Nematov, Dilshod. "Bandgap tuning and analysis of the electronic structure of the Cu<sub>2</sub>NiXS<sub>4</sub> (X= Sn, Ge, Si) system: mBJ accuracy with DFT expense." *Chemistry of Inorganic Materials* 1 (2023): 100001.
47. Kresse G, Furthmuller J. Efficiency of ab-initio total energy calculations for metals and semiconductors using a plane-wave basis set. *Comput. Mater. Sci.* 1996; 6:15–50.
48. Sun, J., Ruzsinszky, A., & Perdew, J. P. (2015). Strongly constrained and appropriately normed semilocal density functional. *Physical review letters*, 115(3), 036402.
49. Sahni, Virah, K-P. Bohnen, and Manoj K. Harbola. "Analysis of the local-density approximation of density functional theory." *Physical Review A* 37.6 (1988): 1895.
50. Perdew, John P., Kieron Burke, and Matthias Ernzerhof. "Generalized gradient approximation made simple." *Physical review letters* 77.18 (1996): 3865.
51. Painter, G. S. "Improved correlation corrections to the local-spin-density approximation." *Physical Review B* 24.8 (1981): 4264.
52. Singh, David J. "Electronic structure calculations with the Tran-Blaha modified Becke-Johnson density functional." *Physical Review B* 82.20 (2010): 205102.
53. Beraich, M., et al. "Experimental and theoretical study of new kesterite Cu<sub>2</sub>NiGeS<sub>4</sub> thin film synthesized via spray ultrasonic technic." *Applied Surface Science* 527 (2020): 146800.
54. Chen, Rongzhen, and Clas Persson. "Electronic and optical properties of Cu<sub>2</sub>XSnS<sub>4</sub> (X= Be, Mg, Ca, Mn, Fe, and Ni) and the impact of native defect pairs." *Journal of Applied Physics* 121.20 (2017).
55. Deepika, R., and P. Meena. "Preparation and characterization of quaternary semiconductor Cu<sub>2</sub>NiSnS<sub>4</sub> (CNTS) nanoparticles for potential solar absorber materials." *Materials Research Express* 6.8 (2019): 0850b7.
56. Kamble, Anvita, et al. "Synthesis of Cu<sub>2</sub>NiSnS<sub>4</sub> nanoparticles by hot injection method for photovoltaic applications." *Materials Letters* 137 (2014): 440-443.
57. Qiu, Xiaofeng, et al. "From unstable CsSnI<sub>3</sub> to air-stable Cs<sub>2</sub>SnI<sub>6</sub>: A lead-free perovskite solar cell light absorber with bandgap of 1.48 eV and high absorption coefficient." *Solar Energy Materials and Solar Cells* 159 (2017): 227-234.
58. Zafar, M., et al. "Theoretical study of structural, electronic, optical and elastic properties of Al<sub>x</sub>Ga<sub>1-x</sub>P." *Optik* 182 (2019): 1176-1185.
59. Johnson, Curtis C., and Arthur W. Guy. "Nonionizing electromagnetic wave effects in biological materials and systems." *Proceedings of the IEEE* 60.6 (1972): 692-718.
60. Jia, Zirui, et al. "MOF-derived Ni-Co bimetal/porous carbon composites as electromagnetic wave absorber." *Advanced Composites and Hybrid Materials* 6.1 (2023): 28.

61. Qian, Sai-Bo, et al. "Lightweight, self-cleaning and refractory FeCo@MoS<sub>2</sub> PVA aerogels: from electromagnetic wave-assisted synthesis to flexible electromagnetic wave absorption." *Rare Metals* 42.4 (2023): 1294-1305.
62. Kortüm, Gustav. *Reflectance spectroscopy: principles, methods, applications*. Springer Science & Business Media, 2012.
63. Modest, Michael F., and Sandip Mazumder. *Radiative heat transfer*. Academic press, 2021.
64. Schäfer, W., and Rudolf Nitsche. "Tetrahedral quaternary chalcogenides of the type Cu<sub>2</sub>IIIIVS<sub>4</sub> (Se<sub>4</sub>)." *Materials Research Bulletin* 9.5 (1974): 645-654.
65. Mani, J., et al. "Tuning the structural, optical, thermal, and electrical properties of Cu<sub>2</sub>NiSnS<sub>4</sub> through cobalt doping for thermoelectrical applications." *Journal of Solid State Chemistry* 326 (2023): 124233.
66. Khatun, Most Marzia, Adnan Hosen, and Sheikh Rashel Al Ahmed. "Evaluating the performance of efficient Cu<sub>2</sub>NiSnS<sub>4</sub> solar cell—A two stage theoretical attempt and comparison to experiments." *Heliyon* (2023).
67. Kolhe, Pankaj, et al. "Study of physico-chemical properties of Cu<sub>2</sub>NiSnS<sub>4</sub> thin films." *Modern Physics Letters B* 37.16 (2023): 2340007.
68. Davlatshoevich, N. D., Islomovich, M. B., Temurjonovich, Y. M., & Tagoykulovich, K. K. (2023). Optimization Optoelectronic Properties Zn<sub>x</sub>Cd<sub>1-x</sub>Te System for Solar Cell Application: Theoretical and Experimental Study. *Biointerface Research in Applied Chemistry*, 13(1).
69. El Khouja, Outman, et al. "Growth and characterization of Cu–Ni–Sn–S films electrodeposited at different applied potentials." *Journal of Materials Science: Materials in Electronics* 34.8 (2023): 760.
70. Nizomov, Z., Asozoda, M., & Nematov, D. (2023). Characteristics of Nanoparticles in Aqueous Solutions of Acetates and Sulfates of Single and Doubly Charged Cations. *Arabian Journal for Science and Engineering*, 48(1), 867-873.

**Disclaimer/Publisher's Note:** The statements, opinions and data contained in all publications are solely those of the individual author(s) and contributor(s) and not of MDPI and/or the editor(s). MDPI and/or the editor(s) disclaim responsibility for any injury to people or property resulting from any ideas, methods, instructions or products referred to in the content.